Investigation of LHCD Efficiency and Transformer Recharging in the EAST Tokamak

2012 Plasma Sci. Technol. 14 201

(http://iopscience.iop.org/1009-0630/14/3/04)

Plasma Science and Technology, Vol.14, No.3, Mar. 2012

Investigation of LHCD Efficiency and Transformer Recharging in the EAST Tokamak*

LI Miaohui (李妙辉), DING Bojiang (丁伯江), LI Wenke (李文科),
KONG Erhua (孔二华), SHAN Jiafang (单家方), LIU Fukun (刘甫坤),
WANG Mao (王茂), XU Handong (徐昱东)

Institute of Plasma Physics, Chinese Academy of Sciences, Hefei 230031, China

Abstract The efficiency of lower hybrid current drive (LHCD) for limiter and divertor configurations in the EAST tokamak is investigated using hot electrical conductivity theory and experimental formulas. The results indicate that the efficiency of current drive in divertor geometry is slightly higher than that in limiter one. To interpret the experimental results, the GENRAY code is applied to calculate the propagation and absorption of the lower hybrid wave (LHW) in different configurations. The numerical results show that the variation in the parallel refractive index ($N_{//}$) between the two configurations is quite large. Transformer recharging experiments were also successfully conducted in EAST. By means of the Karney-Fisch method, the absorption index (α) and the upshift factor of refraction (β) for the LHW are obtained. In addition, the maximum recharging efficiency in EAST is about 4% in the divertor configuration, with a line-averaged electron density of $n_{\mathrm{e\_av}} = 0.7\times10^{19}$ m^{-3}.

Keywords: LHCD, CD efficiency, configuration, transformer recharging

PACS: *52.50, 52.65, 52.40.D*

DOI: 10.1088/1009-0630/14/3/04

1 Introduction

Since the theory of radio frequency (RF) current drive in plasma was proposed by N. J. Fisch in 1978, both theoretical and experimental studies of lower hybrid current drive (LHCD) have been developed rapidly. As one of the most efficient methods to drive non-inductive current, LHCD has been applied in many tokamaks around the world, such as Alcator C-Mod, FTU, TRIAM-1M, JET, JT-60U, Tore Supra, HT-7 and EAST. Generally speaking, the lower hybrid wave (LHW) is capable of providing the required off-axis current drive for advanced tokamak studies of steady-state operation, as well as for saving volt-seconds in the current ramp-up phase [1]. It can also be used to obtain H-mode discharges [2] and to establish an internal transport barrier [3]. An LHCD system in ITER, with 20 MW/5 GHz is now being built up. With its application, a steady-state scenario, namely $Q\sim7$ at $I_{\mathrm{p}}=8.5$ MA over 3000 s, could be expected [1]. However, the density limit problem [4,5], where LHW may not penetrate the plasma core because of plasma density fluctuations and parametric decay instabilities (PDI), is a challenge for LHCD in ITER since the density in the peripheral plasma in ITER is relatively high ($n_{\mathrm{e\_0.8}}\approx0.7\sim1\times10^{20}$ m^{-3} at the normalized minor radius of $r/a=0.8$, and a similar value at the magnetic axis) [6]. Several studies clearly highlight the degradation of current drive (CD) efficiency at lower densities than those necessary for ITER. In JET, LHW cannot penetrate into the plasma core with a plasma edge density of $n_{\mathrm{e\_0.8}}\approx0.3\times10^{20}$ m^{-3} (and $n_{\mathrm{e0}}\approx0.5\times10^{20}$ m^{-3}) [7]. In the early FTU experiments, LHCD was seen only up to a line-averaged density of $n_{\mathrm{e\_av}}\approx1.3\times10^{20}$ m^{-3} and edge density of $n_{\mathrm{e\_0.8}}\approx0.4\times10^{20}$ m^{-3} [8]. Similarly, experiments in ASDEX showed that CD efficiency already became weaker for $n_{\mathrm{e\_av}}\approx0.25\times10^{20}$ m^{-3} [9]. Fortunately, encouraging progress has been achieved recently, indicating that in the ITER range of density ($n_{\mathrm{e\_av}}\geq0.8\times10^{20}$ m^{-3}) for the steady state, the degradation of CD efficiency is negligible [10], and furthermore new experiments performed in FTU with a high electron temperature in the plasma periphery (roughly $T_{\mathrm{e}}\geq0.2$ keV at $r/a=0.8$) suggested that LHW can penetrate into the plasma core at a reactor-grade density, resulting in current drive in the plasma core. The LHCD effects indicated by the considerable increase in hard X-ray emission are observed in FTU even at $n_{\mathrm{e0}}\approx5\times10^{20}$ m^{-3}, $n_{\mathrm{e\_av}}\approx2\times10^{20}$ m^{-3} and $n_{\mathrm{e\_0.8}}\approx0.85\times10^{20}$ m^{-3}, which have so far been considered the upper limit for LHCD operation [6].

CD efficiency is a critical physical quantity in LHCD experiments, and its value is determined by electron density, toroidal magnetic field, LHW parallel refraction index, electron temperature, plasma geometry, and so on [11~14]. Related experiments have been carried out in Tore Supra [15] and PBX-M [16] to study the ef-

*supported by National Natural Science Foundation of China (Nos. 10875149, 10928509 and 10805057) and the National Magnetic Confinement Fusion Science Program of China (No. 2010GB105004)

fect of different configurations on CD efficiency.

This paper is arranged as follows. In section 2 a brief description of the experiments is given. In section 3 the LHCD efficiency in different configurations is presented as investigated experimentally and simulatively, followed by an examination of transformer recharging using LHCD. The final section contains our conclusions.

2 Experimental description

EAST (with a major radius of 1.86 m and a minor radius of 0.44 m) is a fully superconducting tokamak with the flexibility of a double or single null divertor and limiter configurations. The missions of the EAST tokamak are to realize long duration discharge (1000 s) with the help of non-inductive current drive and to explore advanced plasma configuration scenarios. The present LHCD system in EAST operates at $f = 2.45$ GHz and consists of 20 main multi-junction waveguides arranged in an array of 5 rows and 4 columns (one main waveguide consists of four subwaveguides). In this study, all of the experiments (with limiter and divertor geometry) have been conducted with an LHW parallel refraction index of $N_{//}^{\rm peak} = 2.1$ and a toroidal magnetic field of $B_{\rm t} = 2.0$ T.

3 Comparison of LHCD efficiency in different configurations

3.1 Experimental results and analysis

The experimental current drive efficiency is defined as

$$\eta_{\rm exp} = \frac{I_{\rm rf} n_{\rm e\_av} R}{P_{\rm in}}, \tag{1}$$

where $I_{\rm rf}$ is the plasma current driven by LHW, $n_{\rm e\_av}$ is the line averaged density, R is the major radius of the plasma, and $P_{\rm in}$ is the injected LHW power. Only when the loop voltage reaches zero (i.e. the plasma current is fully driven by LHW), can the CD efficiency be obtained from formula (1). However, the loop voltage doesn't reach zero in the usual LHCD experiments. It is therefore necessary to introduce another method to estimate CD efficiency. According to Fisch's hot electric conductivity theory [17], the total plasma current in the case of a non-zero loop voltage can be expressed as

$$I_{\rm p} = I_{\rm ohm} + I_{\rm rf} + I_{\rm hot}, \tag{2}$$

where $I_{\rm ohm} = V/R_{\rm sp}$ is the pure ohmic part and $R_{\rm sp}$ is the Spitzer resistance, $I_{\rm rf} = P_{\rm in}\eta_0/n_{\rm e\_av}R$ is the non-inductive part driven by LHW when $V = 0, \eta_0$ is the fully non-inductive CD efficiency, $I_{\rm hot} = V/R_{\rm hot}$ is the first cross-term and $R_{\rm hot}$ is the hot resistance, inversely proportional to $\int \sigma_{\rm hot} {\rm d}s$. The higher order cross-terms resulting from both RF power and loop voltage are neglected in Eq. (2). Since most LHCD experiments are performed at a constant plasma current, the loop voltage should drop correspondingly when the LHW power is injected. Assuming that the Spitzer resistance keeps constant, the total loop voltage drop is defined as

$$-\frac{\Delta V}{V_{\rm ohm}} = \frac{V_{\rm ohm} - V}{V_{\rm ohm}} = \frac{I_{\rm p} - I_{\rm ohm}}{I_{\rm p}}, \tag{3}$$

where $V_{\rm ohm}$ is the loop voltage in the ohmic phase. Combining Eqs. (2) and (3), we can obtain

$$-\frac{\Delta V}{V_{\rm ohm}} = 1 - \frac{1 - \eta_0 \frac{P_{\rm in}}{n_{\rm e\_av} I_{\rm p} R}}{1 + \frac{\sigma_{\rm hot}}{\sigma_{\rm sp}}}. \tag{4}$$

Defining $P_{\rm norm} = P_{\rm in}/n_{\rm e\_av} I_{\rm p} R$ and $\eta_1 = \sigma_{\rm hot}/(P_{\rm norm}\sigma_{\rm sp})$, Eq. (4) becomes

$$-\frac{\Delta V}{V_{\rm ohm}} = \frac{(\eta_0 + \eta_1) P_{\rm norm}}{1 + \eta_1 P_{\rm norm}}, \tag{5}$$

where $P_{\rm norm}$ is the normalized LHW power, η_1 is the CD efficiency caused by fast electron hot electrical conductivity, $\sigma_{\rm hot}$ is the fast electron hot electrical conductivity and $\sigma_{\rm sp}$ is the Spitzer conductivity.

Following Eq. (5), by means of a simple two parameter least squares fit, we can get η_0 and η_1 simultaneously, even if the data at $-\Delta V/V_{\rm ohm} = 1$ are missing. The obtained results of η_0 and η_1 in limiter and divertor configurations are shown in Figs. 1 and 2, where the dots represent the experimental data and the curves denote the fitting results of Eq. (5). It is shown that η_0 (in units of 10^{19} A $\cdot$ W$^{-1} \cdot$ m^{-2}) in the limiter and divertor configurations are $\eta_0^{\rm Lim} = 0.493 \pm 0.020$, $\eta_0^{\rm Div} = 0.804 \pm 0.025$, with a line averaged density of $n_{\rm e\_av} = 0.7 \times 10^{19}$ m^{-3} and $\eta_0^{\rm Lim} = 0.587 \times 0.079$, $\eta_0^{\rm Div} = 0.830 \pm 0.020$ with $n_{\rm e\_av} = 1.3 \times 10^{19}$ m^{-3}. It is clearly seen that the CD efficiency is higher in a divertor configuration than in a limiter configuration with two different line averaged densities. Similar experimental results were observed in the PBX-M tokamak with the hot electrical conductivity method [16]. By comparing Figs. 1 and 2, a conclusion can be drawn that CD efficiency increases with an increasing density at the present density range. The explanations may be as follows, and the theoretical CD efficiency is given by [18]

$$\eta_{\rm theo} = \frac{310}{\log\Lambda} \frac{4}{(Z_{\rm eff} + 5)} \frac{\alpha}{N^2{}_{//\rm abs}}, \tag{6}$$

where $\log\Lambda$ is the Coulomb logarithm, $Z_{\rm eff}$ is the effective charge number, α is the LHW absorption index and $N_{//\rm abs} = \beta N_{//0}$ is the absorption value of $N_{//}$ by electrons. Although the quantity of density is not involved in formula (6), the effective charge number $Z_{\rm eff}$ is reversely proportional to the density. The variation in $n_{\rm e}$ results in a change to the effective charge number $Z_{\rm eff}$, which is associated with the impurity concentration. A more detailed discussion of density dependence on CD efficiency can be found in Ref. [12]. In order to calculate the CD efficiency η_0 at $V_{\rm loop} = 0$, fully non-inductive current drive experiments in the limiter and divertor configurations were also performed in EAST. Fig. 3 shows two typical waveforms of full-wave current drive with the same line averaged density of $n_{\rm e\_av} = 0.7 \times 10^{19}$ m^{-3}. It is seen that during the full-wave current drive phase, the magnetic flux keeps constant and the loop voltage almost decreases to zero, i.e. the plasma current is sustained only by LHW. Note that in a limiter configuration, to drive a 200 kA plasma current, 750 kW LHW power was injected, whereas a higher plasma current of 250 kA was fully sustained by only 550 kW LHW power in a divertor configuration. Assuming the LHW absorption index $\alpha = 0.75$ (i.e. $P_{\rm in} = \alpha P_{\rm LH}$, where $P_{\rm LH}$ is the launched LHW power), the value of CD efficiency at $V_{\rm loop} = 0$ calculated by expression (1) is $\eta_0^{\rm Lim} = 0.485$ and $\eta_0^{\rm Div} = 0.798$. Such results are in agreement with the previous methods of estimation shown in Figs. 1 and 2.

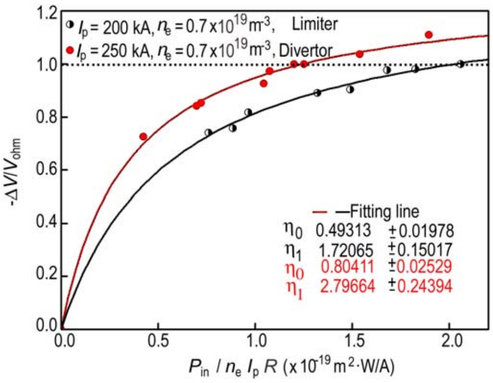

Fig.1 A comparison of LHCD efficiency in limiter and divertor configurations with a line averaged density of $n_{\rm e\_av} = 0.7 \times 10^{19}$ m^{-3} (color online)

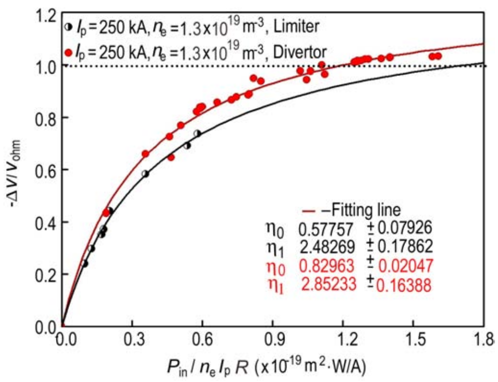

Fig.2 A comparison of LHCD efficiency in limiter and divertor configurations with a line averaged density of $n_{\rm e\_av} = 1.3 \times 10^{19}$ m^{-3} (color online)

Fig. 4 shows the loop voltage variation versus LHW power scan, where all of the discharges are performed with equivalent plasma current and electron density. From the figure we can see that the relation between the decrease in loop voltage and LHW power is nonlinear. This conclusion holds true especially for the loop voltage around zero, i.e. the loop decrease becomes insensitive to the wave power. The reason for this is linked to hot electrical conductivity. According to formula (2), it is known that the total voltage drop $\Delta V_{\rm tot}$ is made up of a part, $\Delta V_{\rm rf}$, and an additional part, $\Delta V_{\rm hot}$ (i.e. $\Delta V_{\rm tot} = \Delta V_{\rm rf} + \Delta V_{\rm hot}$). The computed voltage drop is represented in Fig. 5 [17] as a function of the normalized power, where $\Delta V_{\rm rf}$ is proportional to $P_{\rm norm}$ and is independent of the loop voltage. However, the contribution of the hot conductivity to the voltage drop disappears for $P_{\rm norm} = 0$ and $V_{\rm loop} = 0$, and is at its maximum between the former conditions. According to Ref. [17], the hot conductivity is proportional to $P_{\rm LH}$ (i.e. $\sigma_{\rm hot} \propto P_{\rm LH}$) and a relation of $I_{\rm hot} = V/R_{\rm hot}$ exists. With the increase in $P_{\rm LH}$, $\sigma_{\rm hot}$ is enhanced, whereas $V_{\rm loop}$ would decrease, and as a result the maximum value of $\Delta V_{\rm tot}$ is obtained in the middle of the $P_{\rm norm}$ axis.

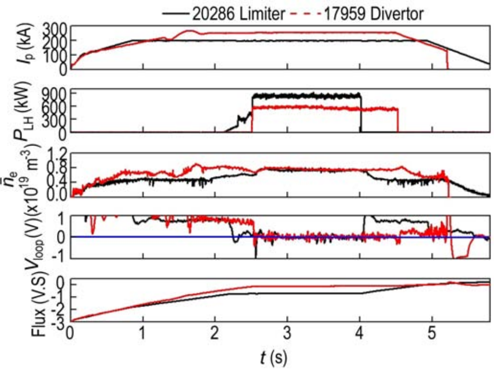

Fig.3 Two typical waveforms of full-wave current drive in the limiter and divertor configurations with a line averaged density of $n_{\rm e\_av} = 0.7 \times 10^{19}$ m^{-3} (color online)

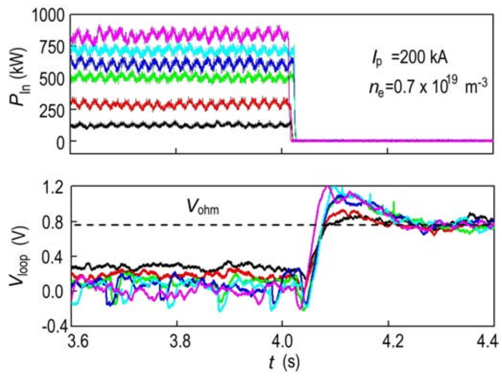

Fig.4 The measured decrease in loop voltage versus time for increasing LHW power levels (color online)

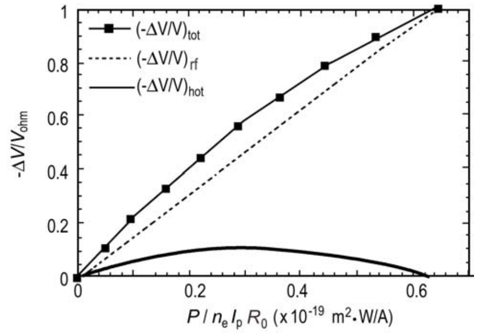

Fig.5 The computed loop voltage drop versus normalized power

3.2 Simulation results and analysis

In order to investigate the effect of the magnetic configuration on CD efficiency in detail, the GENRAY [18] code is used to simulate the propagation and absorption of LHW at different configurations in EAST. GENRAY is a general ray-tracing code for the calculation of electromagnetic wave propagation and absorption in the geometrical optics approximation. It provides a solution to the ray-tracing equations in general non-axisymmetric geometry. Although the validity of the geometrical optics (WKB) is questionable when the wavelength is large, full-wave simulations have shown that the ray-tracing approach gives a satisfactory description of wave propagation at least in a few cases [19]. The magnetic configurations used for the calculation are obtained by using the EFIT code [20], as shown in Fig. 6. For both of the configurations, the temperature and electron density profiles are given by

$$T_{\rm e,i}(r) = (T_{\rm e0,i0} - T_{\rm ea,ia})(1-(r/a)^2)^2 + T_{\rm ea,ia}, \quad (7)$$

$$n_{\rm e}(r) = (n_0 - n_a)(1-(r/a)^2)^2 + n_a, \quad (8)$$

where $T_{\rm e0} = 1.5$ keV, $T_{\rm i0} = 1.0$ keV and $n_0 = 2 \times 10^{19}$ m^{-3}. The effective charge number $Z_{\rm eff}$ is assumed to be constant at 3 throughout the plasma cross-section. In addition, the global parameters are as follows: major radius $R = 1.86$ m, minor radius $a = 0.44$ m, toroidal magnetic field $B_{\rm t} = 2.0$ T, plasma current $I_{\rm p} = 250$ kA, injected refractive index $N_{//0} = 2.1$ and launched power $P_{\rm LH} = 750$ kW. The modeling results of wave propagation and $N_{//}$ variation calculated by the GENRAY code are presented in Fig. 7.

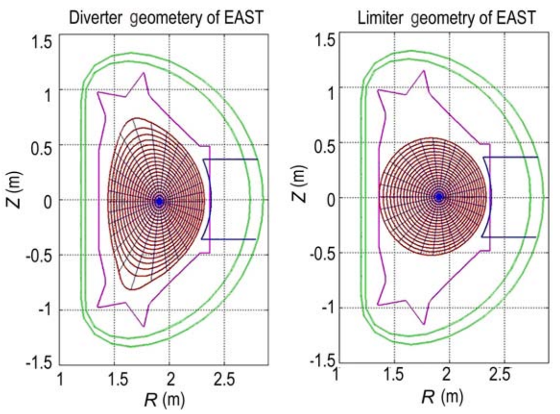

Fig.6 Two magnetic configurations of EAST, with a major radius of $R = 1.86$ m, a minor radius of $a = 0.44$ m, and an elongation of $\kappa = 1.8$ (for the divertor configuration) (color online)

The magnetic configuration is indeed critical for LH wave dynamics, which is also discussed in reference [21]. First, it has an influence on LH wave propagation, since the dispersion relation involves the local magnetic field value, which is illustrated by Fig. 7(a) and (d). In a limiter configuration, the ray trajectory is almost symmetrically distributed throughout the poloidal cross-section, while in the divertor phase the ray propagates mainly between the top and bottom of the chamber. Moreover, the magnetic configuration also plays a crucial role in the variation in the parallel refractive index, hence affecting power deposition and current drive efficiency. In torus coordinates (r, θ, φ), the $N_{//}$ expression is given as [22]

$$N_{//} = \frac{c}{\omega}(\mathbf{k}\cdot\mathbf{B})/\left|\mathbf{B}\right| = \frac{c}{\omega\left|\mathbf{B}\right|}(k_r B_r + \frac{m}{r}B_\theta + \frac{n}{R}B_\varphi), \quad (9)$$

where B_θ is the poloidal field, B_φ is the toroidal field,

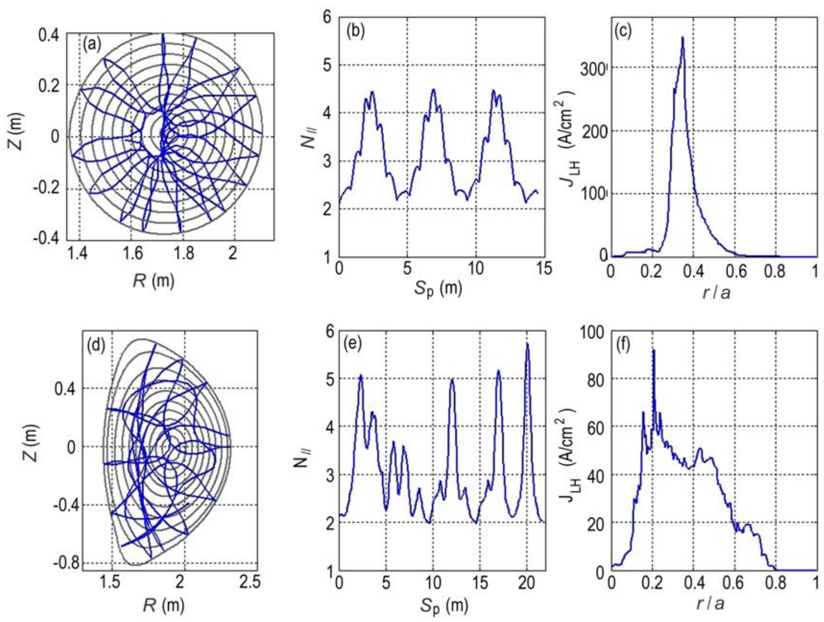

Fig.7 Simulated results of wave propagation and LH current profiles for the limiter and divertor configurations: (a), (d) the poloidal ray trajectory; (b), (e) the variation in parallel refractive index ($N_{//}$) with the poloidal distance of ray trajectory ($s_{\rm p}$); (c), (f) normalized radius profiles of current drive density

m is the poloidal mode number and n is the toroidal mode number. Owing to the toroidal effects, the poloidal mode m should be changed, although the toroidal mode n keeps constant during the wave propagation. From this equation we can see that the variation in $N_{//}$ is mainly related to the local magnetic field B, namely the $N_{//}$ variations should be different in different magnetic configurations, as shown in Fig. 7(b) and (e). It is seen that the $N_{//}$ spectrum is broadened toward the lower bound in diverted plasma, thus resulting in a higher current drive efficiency. However, further studies are required to identify the other mechanisms which have an influence on the CD efficiency, such as the experimental plasma temperature and scrape-off layer (SOL) parameters.

4 Transformer recharging experiments

As is well known, LHW power can be absorbed by resonant electrons, and consequently the toroidal current in tokamaks can be driven effectively. For simplicity, neglecting the effect of hot electrical conductivity to total plasma current, expression (2) yields

$$I_{\rm p} = \frac{V_{\rm loop}}{R_{\rm sp}} + I_{\rm rf}, \tag{10}$$

where $V_{\rm loop}$ is the loop voltage induced by the transformer primary circuit, including an ohmic heating transformer and an equilibrium field transformer. Usually, the experiments are performed at a constant plasma current during LHCD applications, particularly in the EAST tokamak. In this operation scenario there are three statuses during the LHCD period. First, only part of the total current is sustained by LHW. Second, the plasma current is totally maintained by LHW, which is usually called full-wave current drive. In this case the loop voltage is almost kept at zero and the transformer doesn't provide energy for the plasma. When full-wave current drive is realized, if the wave power continues to be increased, the third regime appears, in which only part of the wave power is needed to drive the plasma current and the rest is converted into poloidal electromagnetic energy (i.e. the transformer is recharged by LHCD). In this section, the behavior of power conversion is discussed using the Karney-Fisch theory, which was originally developed to analyze current ramp-up experiments and was subsequently extended to steady regimes [23].

Basically, the theory consists of plotting the dimensionless parameter $P_{\rm el}/P_{\rm in}$ versus $u = \upsilon_{\rm ph}/\upsilon_{\rm r}$. Detailed descriptions of the two parameters are given as follows: $P_{\rm in}$ is the total absorbed wave power by hot electrons ($P_{\rm in} = \alpha P_{\rm LH}$) and $P_{\rm el}$ is the power flowing from these electrons into the poloidal field. These two parameters are related by $P_{\rm el} = -I_{\rm rf} \times V_{\rm loop}$, where $I_{\rm rf}$ can be calculated from the previous CD efficiency η_0 as follows: $I_{\rm rf} = P_{\rm in}\eta_0/n_{\rm e}R$. $\upsilon_{\rm ph}$ is the parallel phase velocity of LHW given by $\upsilon_{\rm ph} = c/(N_{//}\beta)$ and $\upsilon_{\rm r}$ is the electron runaway velocity defined as $\upsilon_{\rm r} = -{\rm sign}(qE)|nq^3 \ln\Lambda/4\pi\varepsilon_0^2 Em|^{1/2}$, where E is the DC electric field and q is the quantity of electric charge. The normalized velocity u reflects the relative importance of the electric field and the collision in slowing down the hot electrons. A function of $G = G(u, Z)$, which gives the correlation between $P_{\rm el}/P_{\rm in}$ and u, is defined as [24]

$$\frac{P_{\rm el}}{P_{\rm in}} = \frac{\partial G}{\partial u}\frac{1}{u}, \tag{11}$$

where Z is the effective ion charge number. By fitting the experimental data, the function can be used to estimate α and β, which are difficult to measure experimentally. Fig. 8 shows two typical discharges of transformer recharging with approximately 1 MW wave power in the limiter and divertor shaped plasma, respectively. It is seen that the magnetic flux decreases suddenly and the loop voltage becomes negative when the power is injected. Now we analyze the data, which are taken for either the limiter or the divertor configuration with two different densities in the Karney-Fisch method. The typical parameters are $I_{\rm p}$= 200 kA, 250 kA, $B_{\rm t}$ = 2.0 T, $N_{//} = 2.1$. To make the best fit, a single constant value of $\alpha = 0.75$ and two values of $\beta_{\rm Lim} = 2.1$ and $\beta_{\rm Div} = 1.67$ (somewhat arbitrarily) are used in this paper, as before. Note that high β indicates low CD efficiency. The experimental data and fit curves for both the limiter and divertor plasma are shown in Fig. 9. The three kinds of values of u ($u < 0, u = 0$ and $u > 0$) correspond to the three LHCD regimes ($I_{\rm rf} < I_{\rm p}, I_{\rm rf} = I_{\rm p}$ and $I_{\rm rf} > I_{\rm p}$) referred to in the preceding text. According to Fig. 9, the lower density data are situated around the $Z_{\rm eff}$ = 5 curve. Meanwhile, for the higher density regime, the data are situated almost between the curves of $Z_{\rm eff} = 2$ and $Z_{\rm eff} = 5$. This is because $Z_{\rm eff}$ is the reverse to the electron density in general. All of the results shown in Fig. 9 prove that the previous assumptions for α and β are reasonable. Finally, the highest energy conversion efficiency ($P_{\rm el}/P_{\rm in}$) obtained in EAST is about 4% in a divertor configuration, with a line-averaged electron density of $n_{\rm e\_av} = 0.7 \times 10^{19}$ m^{-3}.

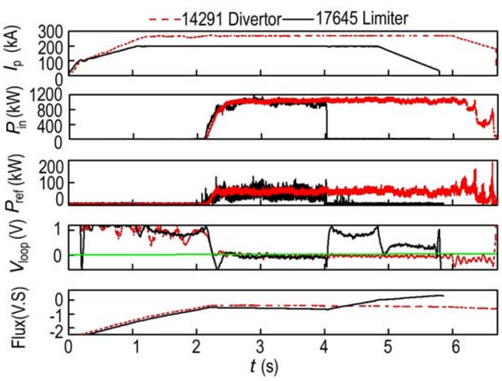

Fig.8 Two typical discharges of transformer recharging in limiter and divertor shaped plasma (color online)

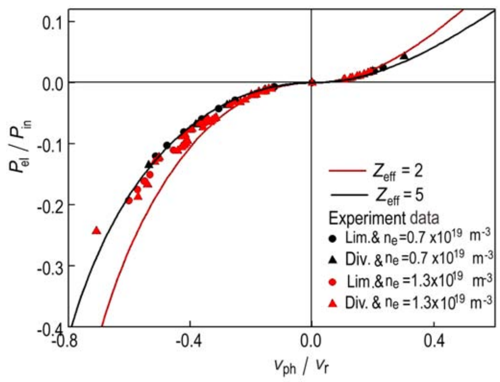

Fig.9 $P_{\rm el}/P_{\rm in}$ versus $\upsilon_{\rm ph}\upsilon_{\rm r}$ for four different regimes (color online)

5 Summary

The CD efficiencies for the limiter and divertor configurations in the EAST tokamak have been investigated using hot electrical conductivity theory and experimental formulas. A comparison of the CD efficiencies in the different configurations shows that they are slightly higher in the divertor configuration than in the limiter phase. The correlation between the decrease in loop voltage and LHW power is also discussed. The modelling results with the GENRAY code indicate that the $N_{//}$ spectrum is broadened toward the lower bound in the diverted plasma, thus resulting in a higher current drive efficiency. In addition, the analysis of transformer recharging in EAST is reported by means of the Karney-Fisch method and a satisfactory fit is obtained. However, all of the experiments are performed with a single refractive index, $N_{//} = 2.1$, and the results are analyzed without taking into account the effect of the relevant plasma parameters, such as the electron temperature profile and SOL conditions, which influence the LHW propagating in the two magnetic configurations differently. Further studies considering the above should be conducted in the future.

Acknowledgments

The authors would like to thank Dr. HARVEY R W from CompX and Dr. SMIRNOV A P from Moscow State University for the code simulation and thank the LHCD task force and EAST team for their contribution to this work.

References

1 Hoang G T, Be'coulet A, Jacquinot J, et al. 2009, Nucl. Fusion, 49: 075001

2 Tsuji S, Ushigusa K, Ikeda Y, et al. 1990, Phys. Rev. Lett., 64: 1023

3 Challis C D, Litaudon X, Tresset G, et al. 2002, Plasma Phys. Control. Fusion, 44: 1031

4 Cesario R, Cardinali A, Castaldo C, et al. 2004, Phys. Rev. Lett., 92: 175002

5 Cesario R, Cardinali A, Castaldo C, et al. 2006, Nucl. Fusion, 46: 462

6 Cesario R, Amicucci L, Cardinali A, et al. 2010, Nature Comm., 1: 55

7 Kirov K K, Baranov Yu, Mailloux J, et al. 2009, LH wave absorption and current drive studies by application of modulated LHCD at JET. Proc. 36th European Phys. Society Conf. on Plasma Physics, Sofia, Bulgaria

8 Gormezano C, Marco F, Mazzitelli G, et al. 2004, Fusion Sci. Technol., 45: 297

9 Pericoli Ridolfini V, Giannone L, Bartiromo R, et al. 1994, Nucl. Fusion, 34: 469

10 Pericoli Ridolfini V, Calabro G, Panaccione L, et al. 2005, Nucl. Fusion, 45: 1386

11 Leuterer F, Soldner F, Mccormick K, et al. 1991, Nucl. Fusion, 31: 2315

12 Ding B J, Kuang G L, Liu Y X, et al. 2000, Chin. Phys. Lett., 17: 519

13 Stevens J E, Bell R E, Bernabei S, et al. 1988, Nucl. Fusion, 28: 217

14 Ushigusa K, Imai T, Ikeda Y, et al. 1989, Nucl. Fusion, 29: 1052

15 Goniche M, Grosman A, Aniel T, et al. 2004, Plasma Phys. Control. Fusion, 46: 913

16 Bernabei S, Cardinali A, Giruzzi G, et al. 1997, Phys. Plasmas, 4: 125

17 Giruzzi G, Barbato E, Bernabei S, et al. 1997, Nucl. Fusion, 37: 673

18 Smirnov A P, Harvey R W. 2003, The GENRAY ray tracing code. Report CompX-2000-01, version 2

19 Wright J C, Bonoli P T, Schmidt A E. 2009, Phys. Plasmas, 16: 072502

20 LAO L L, John H S, Stambaugh R D, et al. 1985, Nucl. Fusion, 25: 1611

21 Ding B J, Qin Y L, Li W K, et al. 2011, Phys. Plasmas, 18: 082510

22 Bonoli P T, Ott E. 1982, Phys. Fluids, 25: 359

23 Karney C F F, Fisch N J, Jobes F C. 1985, Phys. Rev. A, 32: 2554

24 Fisch N J, Karney C F F. 1985, Phys. Rev. Lett., 54: 897

(Manuscript received 9 November 2010)
(Manuscript accepted 5 May 2011)
E-mail address of LI Miaohui: mhli@ipp.ac.cn